ILASS 2008
Sep. 8-10, 2008, Como Lake, Italy

Paper ID ILASS08-5-2

TOTAL TIME FOR SECONDARY BREAKUP OF ELECTRICALLY CHARGED DROPS

Daniel R Guildenbecher, Paul E Sojka

Maurice J. Zucrow Laboratories
School of Mechanical Engineering
Purdue University
West Lafayette, IN 47907-2014
sojka@purdue.edu

ABSTRACT

An experimental investigation was conducted to determine the total breakup time for secondary atomization of electrically charged drops. Results come from movies of breakup in a high speed air stream that were recorded for drops charged to between 0 and 80% of the Rayleigh limit.

The conventional Weber number was found to be insufficient to classify the breakup of charged drops. Rather an electrostatic Weber number was used to account for the presence of the electrostatic surface stress. When the electrostatic Weber number was used in place of the classical Weber number, the observed breakup time scaling was found to be similar to that reported by previous researchers for uncharged drops. It is therefore concluded that secondary breakup of electrically charged drops can be characterized using the wealth of available literature on uncharged Newtonian drops, provided the electrostatic Weber number is used, and that the charge relaxation time is much smaller than the drop breakup time.

INTRODUCTION

Electrostatic sprays have many applications including painting, agricultural sprays, and desorption electrospray ionization (DESI) mass spectrometry [1]. DESI is a promising new technology currently being investigated to perform rapid mass spectrometry for homeland security applications and is the inspiration for this study.

In many spray applications drops encounter regions of high relative velocity which cause them to break apart. Drop fragmentation is due to the disruptive effect of aerodynamic drag, and is termed secondary breakup. This breakup of an already formed drop is in contrast to primary breakup, which refers to the initial formation of drops from a liquid core (either a sheet or jet).

A thorough understanding of secondary breakup phenomena is essential to the design of new spray technologies. Especially important is the relationship between the relative velocity of the surrounding gas to that of the drop breakup process, and the spatial and temporal distribution of drop fragments produced. The first step in gaining this understanding is to develop a quantitative scheme for identifying the time it takes for electrically charged drops to break apart.

The time required for secondary breakup has been extensively studied for uncharged Newtonian drops [2-6]. Pilch and Erdman [2] compiled earlier research results to define three characteristic breakup times. Initiation of breakup is defined as the time elapsed after the drop encounters a high speed air stream and before it begins to significantly deform. Primary breakup time is the time when the initial drop has completely fragmented. Total breakup time is defined as the time after which the initial drop and all fragments have reached a stable state. Of these characteristic times, the total breakup time is the most important to the design of spray applications so this paper will focuses on it.

Pilch and Erdman proposed a best fit correlation for total breakup time based on the Weber (We) and Ohnesorge (Oh) numbers, and on a dimensionless transport time (T):

$$We = \frac{\rho_{gas} U^2 D}{\sigma} \tag{1}$$

$$Oh = \frac{\mu_{liq}}{\sqrt{\rho_{liq} \sigma D}} \tag{2}$$

$$T = t \frac{U \sqrt{\rho_{gas} / \rho_{liq}}}{D} \tag{3}$$

Viscous effects were determined to be negligible for Oh<0.1. This results in the correlations for total breakup time of uncharged drops given in Table 1.

Table 1: Total breakup time for un-charged drops with $Oh < 0.1$ [2]

$T = 6(We-12)^{-0.25}$	$12 < We < 18$
$T = 2.45(We-12)^{0.25}$	$18 < We < 45$
$T = 14.1(We-12)^{-0.25}$	$45 < We < 351$[a]
$T = 0.766(We-12)^{0.25}$	$351 < We < 2670$
$T = 5.5$	$We > 2670$

[a] Pilch and Erdman's paper [2] contains a typo which has been corrected in Table 1.

The conclusions of Pilch and Erdman were confirmed by subsequent researchers [3-6].

While Table 1 can be used to characterize the total breakup time of uncharged drops, there are no reports on how electrostatic charge affects these times. This is surprising since electrostatic charge will migrate to the drop surface for a conductive liquid and create an electrostatic surface stress. This surface stress will oppose the surface tension with the result that charged drops should be less stable when exposed to aerodynamic drag than their electrically neutral counterparts. They can therefore be expected to break up more readily. In addition, charge movement may alter the breakup mechanisms which could further affect the applicability of Table 1 to the secondary breakup of charged drops.

The study described here was performed to investigate the effects of aerodynamic drag on electrically charged drops, to determine total breakup times for charged liquid drops undergoing aerodynamic drag-induced deformation, to propose a correlation scheme for charged drops similar to that of Table 1, and to investigate the effects of varying the liquid conductivity.

This study differs from previous ones that were restricted to the spontaneous breakup of stationary electrically charged drops when they are charged beyond a critical limit because our work demonstrates secondary breakup can occur at drop charge-to-mass ratios well below those for a stationary charged drop.

Previous studies have shown that the maximum charge a stationary drop can sustain is somewhere between 70 and 100% of the Rayleigh limit [7]. This limit, proposed by Lord Rayleigh, occurs when the electrostatic repulsion force equals the consolidating surface tension force:

$$q_{Ra} = \sqrt{8\pi^2 \sigma \varepsilon_0 D^3} \qquad (4)$$

At this point the drop breaks apart [8].

EXPERIMENTAL SETUP

Isopropyl alcohol was selected as the test liquid due to its low viscosity and moderate electrical conductivity. Its relevant physical properties are given in Table 2.

Uniform size drops were created using a stainless steel syringe tip connected to a syringe pump, as shown in Fig. 1. The syringe tip was oriented vertically downward and the flow rate adjusted to achieve steady streams of drops having (adjustable) monodisperse diameters between 0.8 and 1.2 mm.

Table 2: Relevant physical properties for isopropyl alcohol

Density, ρ_{liq}	785 kg/m^3
Surface Tension, σ	0.0228 N/m
Viscosity, μ_{liq} [b]	2.40 mPa s
Conductivity, $\sigma_{e\text{-}liq}$ [c]	6.30 μS/m
Dielectric Constant, κ_{liq} [b]	18.6
Electrical Permittivity, ε_{liq}	1.65x10^{-10} C^2/N m^2

[b] Bottle label (20˚C)

[c] Measured using Hanna Instruments UPWW

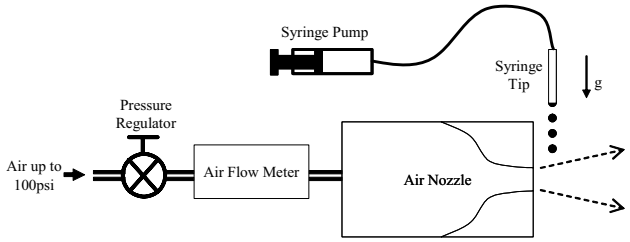

Figure 1: Liquid and air supply systems

The drops were charged by applying a voltage to the syringe tip, as illustrated in Fig. 2. Drop charge was determined by using a Keithley model 610BR picoammeter to measure the current in a liquid collection cup while also measuring the drop production rate using the optical system discussed below. Applied potentials between 0 and 3.6 kV resulted in drops charged between 0 and 80% of the Rayleigh limit. (This setup did not allow drop charging above 80% of the Rayleigh limit.)

The drops were directed downward toward a horizontal high speed air jet created using the air nozzle shown in Fig. 1. This setup is similar to that of Reitz and co-workers [9,10]. The nozzle was designed to suppress boundary layers such that the air jet has a nearly-uniform velocity profile at the nozzle exit. Particle Image Velocimetery (PIV) was used to characterize the steady state air jet. Typical PIV results are shown in Fig. 3. As a check on the PIV measurements, a pitot-static tube was also used to directly measure the jet air speed. The two sets of data agreed to within 20%.

Drop breakup was recorded using a Vision Research Phantom v7 high speed digital camera and an Infinity model K2 long distance microscope. Illumination was achieved by using a Kratos 1000W Xe arc lamp to produce a collimated beam. The beam reflected off a dichroic mirror, which also filtered out IR and UV components. Finally, an opal glass diffuser plate was used to scatter the collimated beam and backlight the drop breakup process. Figure 4 shows the optical arrangement. Using this arrangement, movies of drop breakup were created at 4700 fps with a capture window time of 10 μs, effectively freezing the motion.

A calibration key was created to allow direct measurement of drop diameters from the recorded images. It was also possible to map the PIV results, such as those from Fig. 3, onto the drop motion images such that the air velocity at the drop breakup location could be determined.

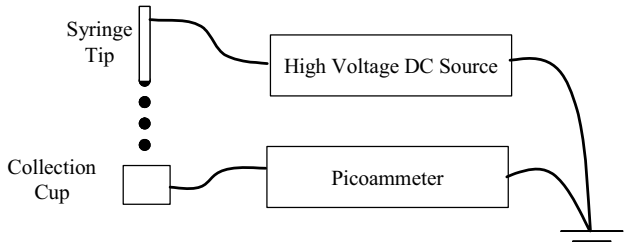

Figure 2: Drop electrostatic charging and measurement apparatus

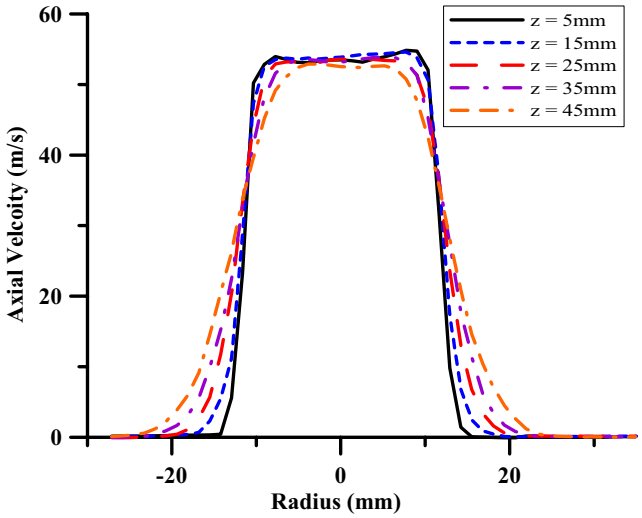

Figure 3: PIV characterization of air jet flowfield

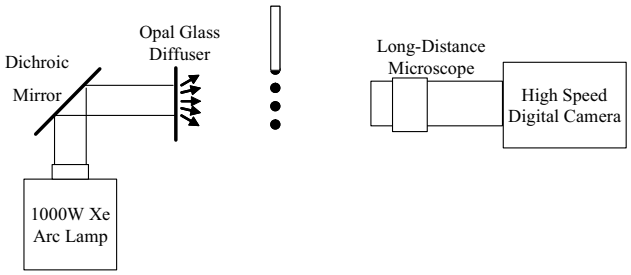

Figure 4: Optical system for capturing drop breakup

RESULTS

The first step in this investigation was to demonstrate that the current experimental setup can reproduce results consistent with those of previous researchers, such as the ones provided in Table 1. This was accomplished by recording breakup of uncharged drops for twelve air speeds (10 to 50 m/s). Fig. 5 contains typical results.

Pilch and Erdman [2] did not specify if their reported total breakup time was measured starting with the instant when the drop enters the air stream, or if the breakup time started after the initiation time. In the current experiment, the results most closely match previous reports when using the latter definition; therefore, the results reported here assume that the total breakup time begins when the drop is deformed into an ellipsoidal shape, as is shown in Fig. 5.

The recorded total breakup times for all uncharged cases are shown in Fig. 6. They agree with previously reported correlations. Also, the amount of scatter in the data is approximately the same as reported in the literature [2].

The next step was to ensure that the breakup behavior observed was due to aerodynamic forces acting on the charged drops. Movies of charged drops taken when the air stream was turned off showed no evidence of breakup whatsoever, even for sampling times much greater than the breakup times reported here. This demonstrates that charged drop breakup behavior reported here is the result of aerodynamic drag acting on the charged drop, and is not the spontaneous breakup of stationary charged drops that has been studied by previous researchers [7,8].

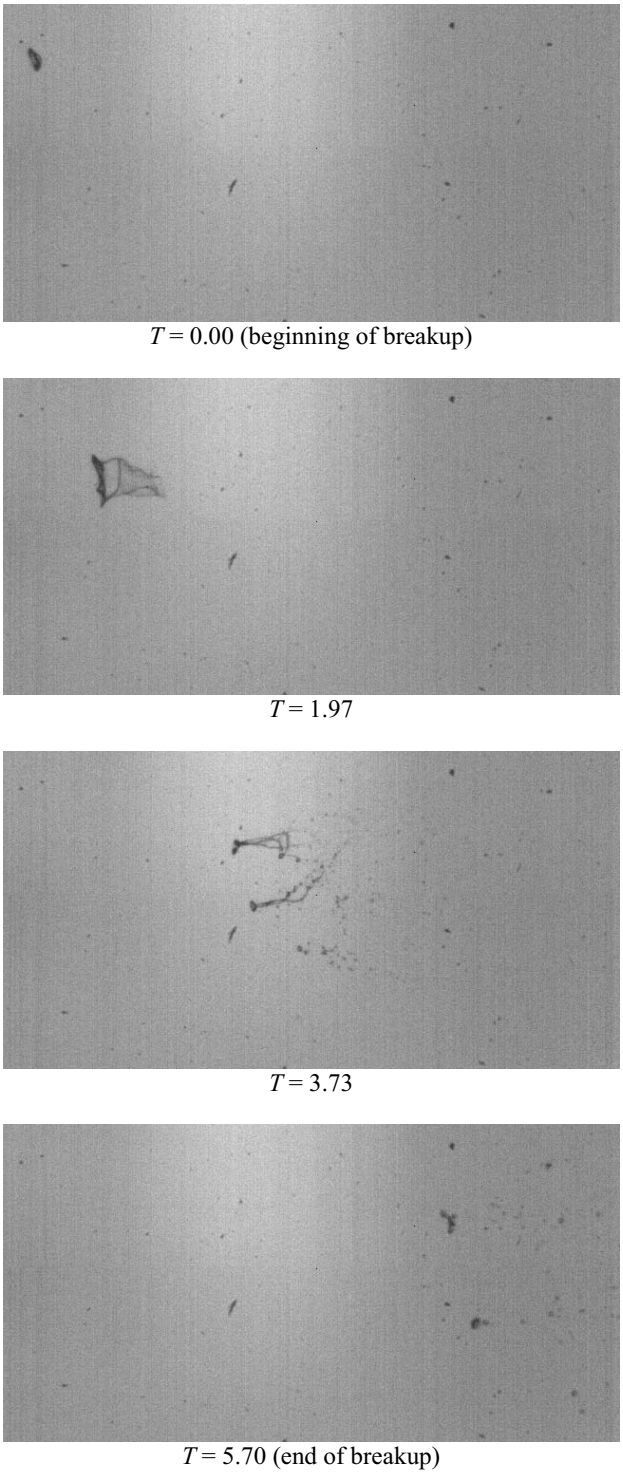

$T = 0.00$ (beginning of breakup)

$T = 1.97$

$T = 3.73$

$T = 5.70$ (end of breakup)

Figure 5: Typical uncharged drop breakup ($We = 45$)

The third step was to evaluate the influence drop evaporation has on the behavior reported here. This was achieved by making movies of uncharged drops falling with the air stream turned off. They demonstrated that the evaporation time is much longer than the breakup times reported here. This indicates that evaporation has no influence on the drop breakups observed and can safely be ignored.

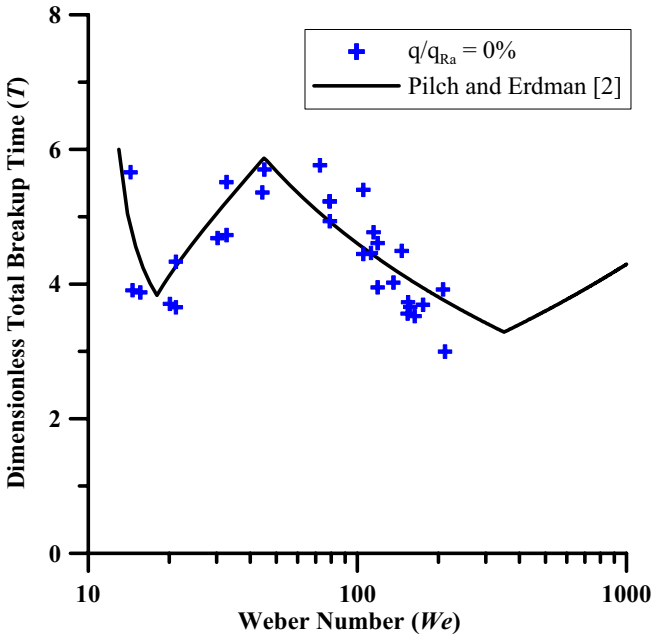

Figure 6: Total breakup time for uncharged drops

After these preliminaries, drop secondary breakup was recorded for twelve air speeds (10 to 50 m/s) and two levels of charge (q/qRa=60% and 80%). In all cases Oh<0.1; therefore the observed breakup behavior was assumed to be independent of viscous effects. This assumption will be tested in a future study.

As expected classical Weber number scaling for total breakup time does not hold when drop charge increases above zero. As an example, compare the breakup behaviour shown in Fig. 7 with Fig. 5, both for $We \approx 50$. As expected the electrostatic charge has reduced the breakup time and changed the breakup morphology.

Because drop charging affects secondary breakup, data were correlated using an "electrostatic" Weber number, We_{e-}, first suggested by Shrimpton and Laoonaul [9]:

$$We_{e-} = \frac{\rho_{air} U^2 D}{\sigma - q^2/8\pi^2\varepsilon_0 D^3} \qquad (5)$$

Here the consolidating surface tension term in the classical Weber number has been modified to account for the opposing electrostatic surface stress. Note that the electrostatic Weber number reduces to its classical counterpart for an uncharged drop. Also note that the electrostatic Weber number becomes infinite when the drop is charged to the Rayleigh limit, indicating drop breakup regardless of relative velocity.

The use of the electrostatic Weber number also necessitates the definition of an "electrostatic" Ohnesorge number, Oh_{e-}:

$$Oh_{e-} = \frac{\mu_{liq}}{\sqrt{\rho_{liq} D\left(\sigma - q^2/8\pi^2\varepsilon_0 D^3\right)}} \qquad (6)$$

In Eq. (6) the surface tension term has once again been modified to account for the opposing electrostatic surface stress. Using Eq. (6) showed that $Oh_{e-}<0.1$ for all cases considered here, so the observed breakup morphology was assumed to be independent of viscous effects. This assumption will be checked in a future study.

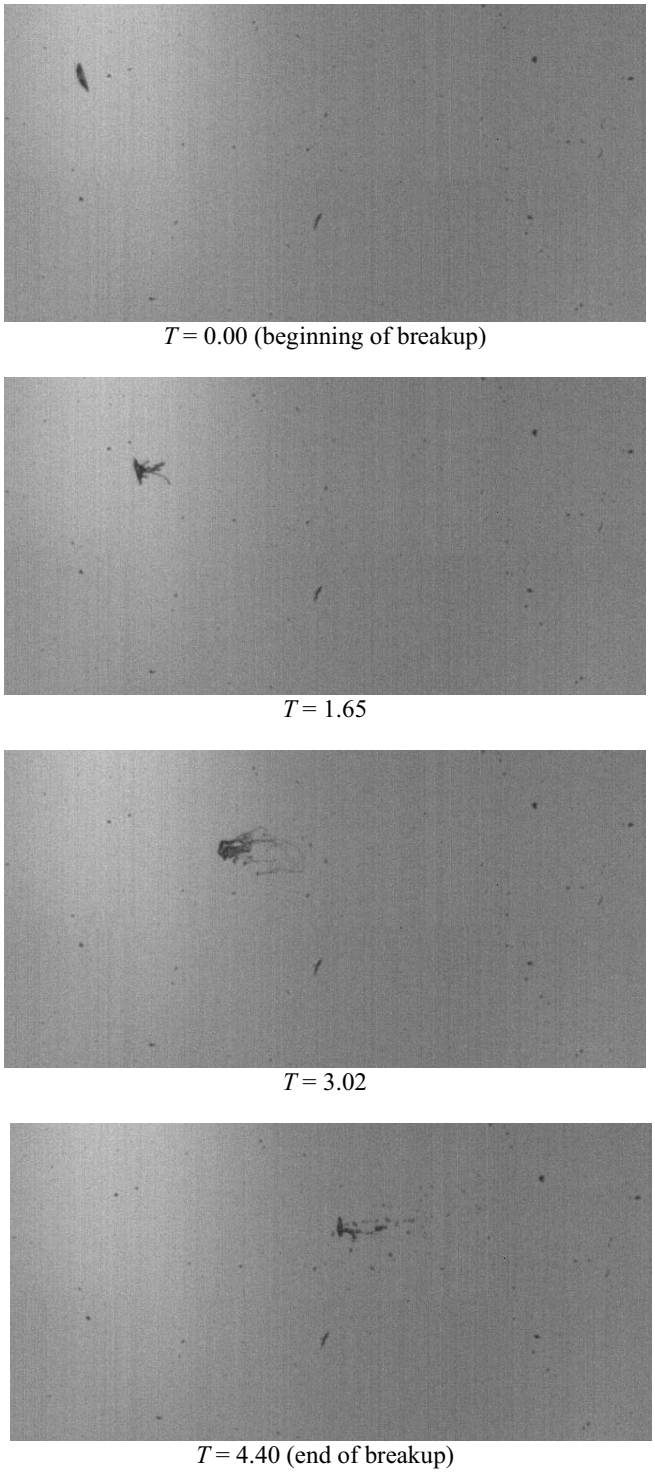

$T = 0.00$ (beginning of breakup)

$T = 1.65$

$T = 3.02$

$T = 4.40$ (end of breakup)

Figure 7: Typical charged drop breakup (q/q_{Ra}=80%, We_{e-}=130, We=50)

For charged drops of isopropyl alcohol, the substitution of the electrostatic We for the classical We was found to be sufficient to correlate the measured total breakup time to the results of previous experiments involving uncharged drops. This is illustrated in Figs. 8 and 9. Figure 8 shows the total breakup time plotted as a function of the classical We. Clearly the correlation no longer holds for charged drops. Figure 9 shows the same data plotted as a function of electrostatic We. The correlation is now much improved.

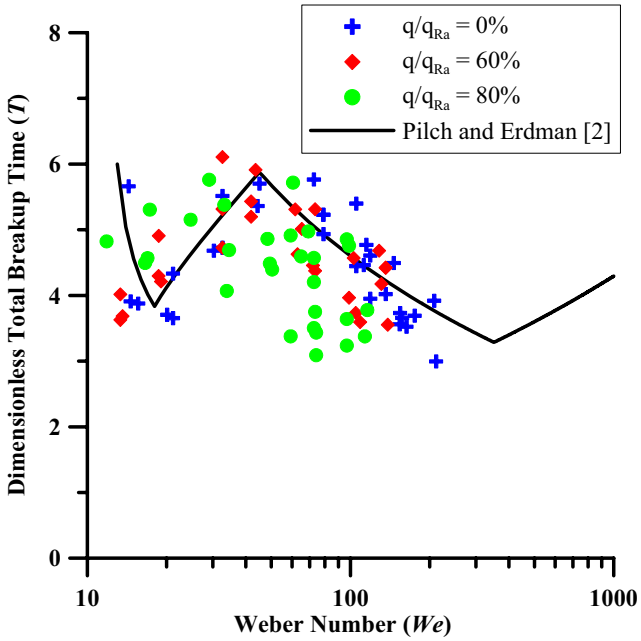

Figure 8: Total breakup time for charged drops (versus classical We)

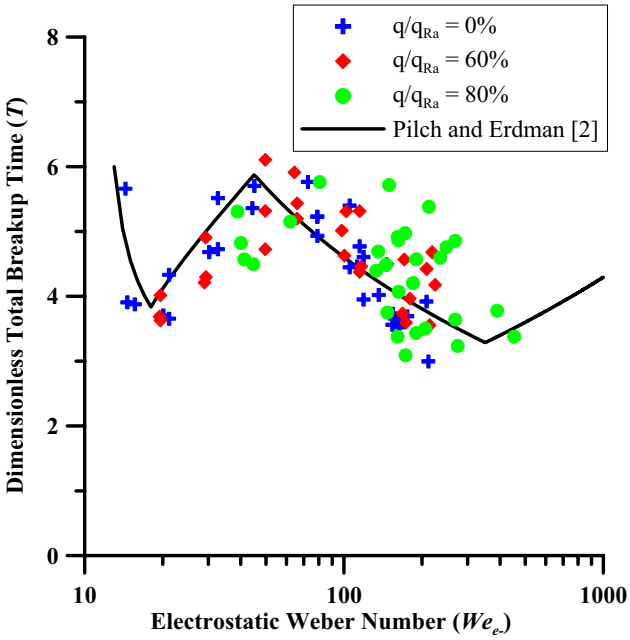

Figure 9: Total breakup time for charged drops (versus electrostatic We)

A key issue is the charge relaxation time, defined as the electrical permittivity divided by the conductivity:

$$\tau_{liq} = \frac{\varepsilon_{liq}}{\sigma_{e-liq}} \qquad (7)$$

The charge relaxation time is an indication of the time required for electrical charge to reach an equilibrium spatial distribution. For isopropyl alcohol τ_{liq}=26 μs, while the movies show drop breakup times to be between 1.5 and 10 ms. This two order of magnitude difference strongly suggests charge redistributes itself over the perturbed drop surface much more rapidly than the surface deforms. Such rapid charge redistribution would result in a spatially uniform electrostatic stress that opposes surface tension equally at all points. This justifies the form of We_{e-} and Oh_{e-} given in Eqns. (5) and (6). As a result, correlations to uncharged results such as Fig. 9 are reasonable.

All of the results presented up to this point are for isopropyl alcohol where the charge relaxation time is short compared to the breakup time. Instances where the charge relaxation time is greater than the drop breakup time will likely require a different approach to analyzing the results.

To study these effects a preliminary investigation was performed using of a mixture of 95% hexane and 5% ethyl alcohol by volume. Such a combination has been shown to have a low electrical conductivity ($\sigma_{e\text{-}liq}$=5x10^{-5} μS/m) and dielectric constant (κ_{liq}=2.0) [10]. This results in a charge relaxation time (τ_{liq}=0.4 s) which is three order of magnitudes greater than the breakup time.

Figs. 10 and 11 show the initial results for the case of slow charge relaxation. Unfortunately, the current experimental setup did not allow drop charges greater than 35% of the Rayleigh charge limit. Consequently any differences between the uncharged and charged cases are within experimental uncertainty and more work is needed.

EXPERIMENTAL UNCERTAINTY

Of importance to this study is the experimental uncertainty in the classical *We*, electrostatic *We*, and total breakup time. The approach of Klein and McClintock [11] was used to calculate the propagation of measurement uncertainties. In doing so all errors were assumed to be random.

The uncertainty in the diameter measurement was determined based on image blur and was found to be ±8% of the measured value. The variation in air velocity was approximated as the standard deviation of the PIV results and was found to be ±10%. The uncertainty in the drop charge was calculated based on an estimated ±10% uncertainty in the drop production rate, resulting in an approximate ±10% uncertainty in the drop charge. The breakup time was determined based on a qualitative judgement of the end of fragmentation, and the uncertainty in the measured time was approximated to be ±10%.

Combining the above uncertainties, the experimental uncertainty for the classical *We* was found to be ±23% of the actual value, while the experimental uncertainty for the electrostatic *We* was found to be ±23% of the actual value. Finally the experimental uncertainty of the non-dimensional total breakup time was found to be ±17%.

SUMMARY AND CONCLUSIONS

An experimental investigation was conducted to determine the total breakup time of electrically charged drops. When the charge relaxation time is much less than the breakup time, the electrostatic Weber number must be used in place of the classical Weber number to correlate total breakup time. When that is done, the wealth of literature on the secondary breakup of uncharged Newtonian drops [2-6] can be used to predict the behavior of charged drops. Further investigation is necessary to identify the limit where this assumption breaks down.

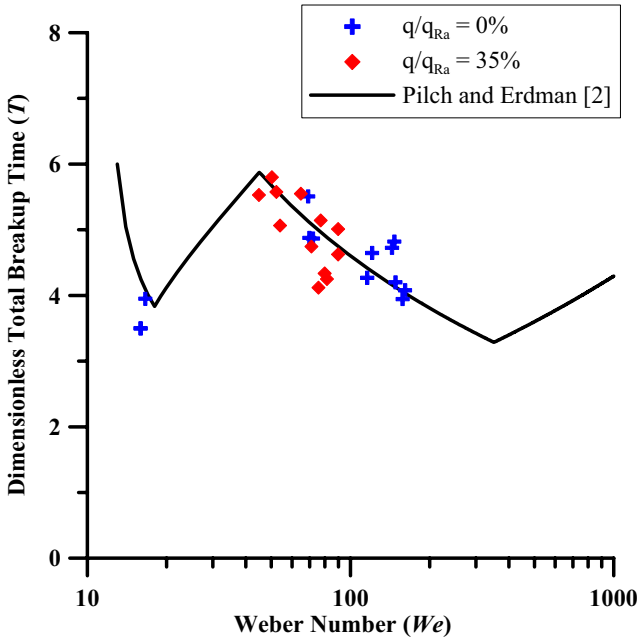

Figure 10: Total breakup time for charged drops of 95% hexane 5% ethyl alcohol (versus classical We)

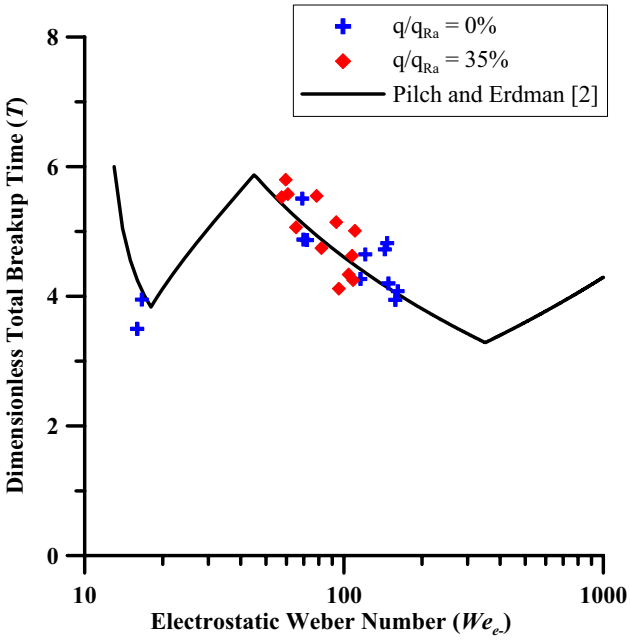

Figure 11: Total breakup time for charged drops of 95% hexane 5% ethyl alcohol (versus electrostatic We)

In the future, low conductivity drops will be studied at higher levels of charge to determine the appropriate breakup time scaling. The effects of drop viscosity on breakup time will also be studied. Finally, measurements will be made of the size, velocity, and charge distributions of fragments after secondary breakup has completed. The overall result will be a complete understanding of charged drop secondary breakup and the ability to design improved spray processes.

ACKNOWLEDGMENT

This material is based upon work supported under a National Science Foundation Graduate Research Fellowship.

NOMENCLATURE

Symbol	Quantity	SI Unit
D	initial drop diameter	m
Oh	Ohnesorge number	dimensionless
Oh_{e-}	electrostatic Ohnesorge number	dimensionless
q	drop charge	C
q_{Ra}	Rayleigh drop charge limit	C
t	total breakup time	s
T	total breakup time	dimensionless
U	gas phase velocity	m/s
We	Weber number	dimensionless
We_{e-}	electrostatic Weber number	dimensionless
ε_0	electrical permittivity of vacuum	$C^2/N\ m^2$
ε_{liq}	liquid electrical permittivity	$C^2/N\ m^2$
κ_{liq}	liquid dielectric constant	dimensionless
μ_{liq}	liquid viscosity	Pa s
ρ_{gas}	gas phase density	kg/m^3
ρ_{liq}	liquid density	kg/m^3

REFERENCES

[1] A. Venter, P.E. Sojka and G. Cooks, Droplet Dynamics and Ionization Mechanisms in Desorption Electrospray Ionization Mass Spectrometry, *Anal. Chem.*, vol. 78, pp. 8549-8555, 2006.

[2] M. Pilch and C.A. Erdman, Use of Breakup Time Data and Velocity History Data to Predict the Maximum Size of Stable Fragments for Acceleration-Induced Breakup of a Liquid Drop, *Int. J. Multiphase Flow*, vol. 13(6), pp. 741-757, 1987.

[3] G.M. Faeth, L.P. Hsiang and P.K. Wu, Structure and Breakup Properties of Sprays, *Int. J. Multiphase Flow*, vol. 21(supp), pp. 99-127, 1995.

[4] W.H. Chou, L.P. Hsiang and G.M. Faeth, Temporal Properties of Drop Breakup in the Shear Breakup Regime, *Int. J. Multiphase Flow*, vol. 23(4), pp. 651-669, 1997.

[5] W.H. Chou and G.M. Faeth, Temporal Properties of Drop Breakup in the Bag Breakup Regime, *Int. J. Multiphase Flow*, vol. 24, pp. 889-912, 1998.

[6] Z. Dai and G.M. Faeth, Temporal Properties of Secondary Drop Breakup in the Multimode Breakup Regime, *Int. J. Multiphase Flow*, vol. 27, pp. 217-236, 2001.

[7] J.S. Shrimpton, Dielectric Charged Drop Break-up at Sub-Rayleigh Limit Conditions, *IEEE Transactions on Dielectrics and Electrical Insulation*, vol. 12(3), pp. 573-578, 2005.

[8] Lord Rayleigh, On the Equilibrium of Liquid Conducting Masses Charged with Electricity, *Phil. Mag.*, vol. 5(14), pp. 184-186, 1882.

[9] J.S. Shrimpton, Y. Laoonual, Dynamics of Electrically Charged Transient Evaporating Sprays, *Int. J. Numer. Meth. Engng.*, vol. 67, pp. 1063-1081, 2006.

[10] M. Zdanowski, S. Wolny, D.O. Zmarzły, T. Boczar, ECT of Ethanol and Hexane Mixtures in the Spinning Disk System, *J. Electrostatics*, vol. 65, pp. 239-243, 2007.

[11] S.J. Klein, F.A. McClintock, Describing Uncertainties in Single-Sample Experiments, *Mechanical Engineering*, vol. 75, pp. 3-8, 1953.